Radioiodinated Styrylbenzenes and Thioflavins as Probes for Amyloid Aggregates

Z.-P. Zhuang,[†] M.-P. Kung,[†] C. Hou,[†] D. M. Skovronsky,[‡] T. L. Gur,[‡] K. Plössl,[†] J. Q. Trojanowski,[‡] V. M.-Y. Lee,[‡,§] and H. F. Kung*[,†,§]

Departments of Radiology, Pathology and Laboratory Medicine, and Pharmacology, University of Pennsylvania, Philadelphia, Pennsylvania 19104

Received February 1, 2001

We report for the first time that small molecule-based radiodiodinated ligands, showing selective binding to Aβ aggregates, cross the intact blood−brain barrier by simple diffusion. Four novel ligands showing preferential labeling of amyloid aggregates of Aβ(1−40) and Aβ(1−42) peptides, commonly associated with plaques in the brain of people with Alzheimer's disease (AD), were developed. Two ^{125}I-labeled styrylbenzenes, (*E*,*E*)-1-iodo-2,5-bis(3-hydroxycarbonyl-4-hydroxy)-styrylbenzene, **12** (ISB), and (*E*,*E*)-1-iodo-2,5-bis(3-hydroxycarbonyl-4-methoxy)styrylbenzene, **13** (IMSB), and two ^{125}I-labeled thioflavins, 2-[4′-(dimethylamino)phenyl]-6-iodobenzothiazole, **18a** (TZDM), and 2-[4′-(4″-methylpiperazin-1-yl)phenyl]-6-iodobenzothiazole, **18b** (TZPI), were prepared at a high specific activity (2200 Ci/mmol). In vitro binding studies of these ligands showed excellent binding affinities with K_d values of 0.08, 0.13, 0.06, and 0.13 nM for aggregates of Aβ(1−40) and 0.15, 0.73, 0.14, and 0.15 nM for aggregates of Aβ(1−42), respectively. Interestingly, under a competitive-binding assaying condition, different binding sites on Aβ(1−40) and Aβ(1−42) aggregates, which are mutually exclusive, were observed for styrylbenzenes and thioflavins. Autoradiography studies of postmortem brain sections of a patient with Down's syndrome known to contain primarily Aβ(1−42) aggregates in the brain showed that both [^{125}I]**18a** and [^{125}I]**18b** labeled these brain sections, but [^{125}I]**13**, selective for Aβ(1−40) aggregates, exhibited very low labeling of the comparable brain section. Biodistribution studies in normal mice after an iv injection showed that [^{125}I]**18a** and [^{125}I]**18b** exhibited excellent brain uptake and retention, the levels of which were much higher than those of [^{125}I]**12** and [^{125}I]**13**. These findings strongly suggest that the new radioiodinated ligands, [^{125}I]**12** (ISB), [^{125}I]**13** (IMSB), [^{125}I]**18a** (TZDM), and [^{125}I]**18b** (TZPI), may be useful as biomarkers for studying Aβ(1−40) as well as Aβ(1−42) aggregates of amyloidogenesis in AD patients.

Introduction

Alzheimer's disease (AD) is a progressive neurodegenerative disorder characterized by cognitive decline, irreversible memory loss, disorientation, and language impairment. Postmortem examination of AD brain sections reveals abundant senile plaques (SPs) composed of amyloid-β (Aβ) peptides and numerous neurofibrillary tangles (NFTs) formed by filaments of highly phosphorylated tau proteins (for recent reviews and additional citations, see ref 1−3). Familial AD (FAD) is caused by multiple mutations in the Aβ precursor protein (APP), presenilin 1 (PS1), and presenilin 2 (PS2) genes. While the exact mechanisms underlying AD are not fully understood, all pathogenic FAD mutations studied thus far increase production of the more amyloidogenic 42−43-amino acid form of the Aβ peptide. Thus, at least in FAD, dysregulation of Aβ production appears to be sufficient to induce a cascade of events leading to neurodegeneration. Indeed, the amyloid cascade hypothesis suggests that formation of extracellular fibrillar Aβ aggregates in the brain may be a pivotal event in AD pathogenesis.[2,4−6] Various approaches in trying to inhibit the production and reduce the extent of accumulation of fibrillar Aβ in the brain are currently being evaluated as potential therapies for AD.[7−12] It is therefore of great interest to develop ligands that specifically bind fibrillar Aβ aggregates. Since extracellular SPs are accessible targets, these new ligands could be used as in vivo diagnostic tools and as probes to visualize the progressive deposition of Aβ in studies of AD amyloidogenesis in living patients.

To this end, several interesting approaches for developing fibrillar Aβ aggregate specific ligands have been reported.[13−20] The most attractive approach is based on highly conjugated chrysamine-G (CG) and Congo red (CR) (see Figure 1), and the latter has been used for fluorescent staining of SPs and NFTs in postmortem AD brain sections.[13,21] The inhibition constants (K_i) for binding to fibrillar Aβ aggregates of CR, CG, and 3′-bromo and 3′-iodo derivatives of CG are 2800, 370, 300, and 250 nM, respectively.[18] These compounds have been shown to bind to Aβ(1−40) peptide aggregates in vitro as well as to fibrillar Aβ deposits in AD brain sections.[18]

The unique interaction between fibrillar Aβ aggregates and small negatively charged, highly conjugated ligands may represent a novel opportunity for designing specific ligands for in vivo imaging of amy-

* To whom correspondence should be addressed: Department of Radiology, University of Pennsylvania, Room 305, 3700 Market St., Philadelphia, PA 19104. Telephone: (215) 662-3096. Fax: (215) 349-5035. E-mail: kunghf@sunmac.spect.upenn.edu.
[†] Department of Radiology.
[‡] Department of Pathology and Laboratory Medicine.
[§] Department of Pharmacology.

10.1021/jm010045q CCC: $20.00
Published on Web 05/04/2001

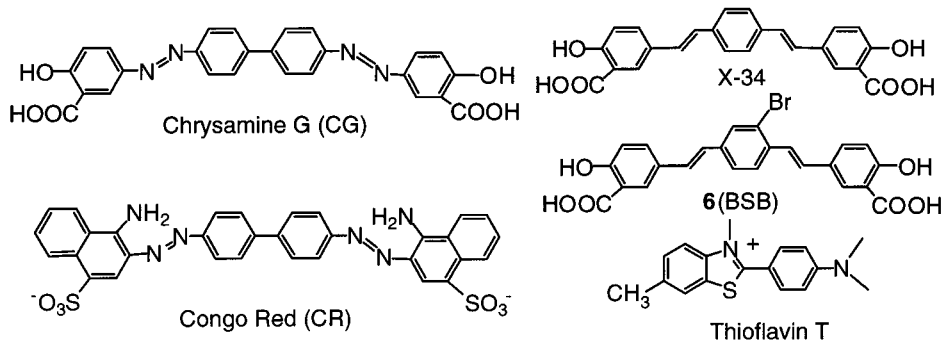

Figure 1. Chemical structures of chrysamine G (CG), Congo Red (CR), X-34, thioflavin T, and **6** (BSB).

loid.[15,16] Tracers labeled with ^{123}I ($T_{1/2}$ = 13 h, 159 keV γ-ray)[18,22−25] or ^{99m}Tc ($T_{1/2}$ = 6 h, 140 keV γ-ray)[20] may be useful as single-photon emission computed tomography (SPECT) imaging agents for detection and eventually quantification of fibrillar Aβ aggregates in the brains of living patients. Initial attempts to develop ^{99m}Tc-labeled CG and CR derivatives were reported.[14,20,26,27] They are too large (molecular weight > 700), making them unlikely candidates for penetrating the intact blood−brain barrier, and therefore, they are not suitable as imaging agents for detecting fibrillar Aβ aggregates in patients with AD. Recently, radiolabeled Aβ peptides have been reported as potential imaging agents;[28,29] however, the usefulness of these peptides as brain imaging agents remains to be investigated.

Recently, a new compound, X-34, has been produced by replacing the diazo group of CG with a simple vinyl group and substituting one phenyl for the biphenyl group (see Figure 1).[30] X-34 showed excellent binding to fibrillar Aβ aggregates, and in postmortem AD brain tissue, it displays intense fluorescent staining associated with SPs and NFTs. Significantly, this substitution has several advantages: (i) decreased molecular weight, which may increase the extent of penetration of tissue; (ii) improved in vitro stability; and (iii) the fact that derivatives could be prepared via a versatile reaction scheme, which is amenable to additional substitution. X-34 is a potentially useful ligand for studying fibrillar Aβ aggregates, but the chemical synthesis of this compound or the iodinated derivatives has not been published. Thus, to develop better and more versatile ligands for studies of fibrillar Aβ aggregates, we initially prepared a bromo derivative, **6** (BSB), which displayed exquisite properties as a novel fluorescent probe for highly specific labeling of fibrillar Aβ aggregates.[31] BSB labels Aβ plaques in human AD brain sections with high sensitivity and specificity, and it permeates living cells in culture and binds specifically to intracellular Aβ aggregates. Additionally, it crosses the blood−brain barrier and labels numerous AD-like Aβ plaques (as detected by fluorescence) throughout the brain of transgenic mice following iv injection. To characterize **6** (BSB) further, we prepared the corresponding ^{125}I-labeled derivatives **12** (ISB) and **13** (IMSB).

Potential ligands for detecting Aβ aggregates in the living brain must cross the intact blood−brain barrier. Thus, brain uptake can be improved by using ligands with a smaller molecular size and increased lipophilicity. To generate ligands with those properties, we looked to highly conjugated thioflavins S and T, which are commonly used as dyes for staining the Aβ aggregates in the AD brain.[32] These compounds are known to bind amyloid specifically. Similar series of thioflavin compounds have been reported as potential antitumor agents.[33,34] They are based on benzothiazole, which is relatively small in molecular size. However, the thioflavins contain an ionic quaternary amine, which is permanently charged and unfavorable for brain uptake. Thus, two neutral derivatives of thiazoles, 2-[4′-(dimethylamino)phenyl]-6-iodobenzothiazole, **18a** (TZDM), and 2-[4′-(4″-methylpiperazin-1-yl)phenyl]-6-iodobenzothiazole, **18b** (TZPI), were designed as potential ligands for imaging Aβ aggregates in the AD brain.

Reported herein are syntheses and initial characterization of these novel radioiodinated ligands, [^{125}I]**12** (ISB), [^{125}I]**13** (IMSB), [^{125}I]**18a** (TZDM), and [^{125}I]**18b** (TZPI), as selective probes that are useful for detecting amyloid aggregates in the brain by in vivo and in vitro techniques.

Results and Discussion

The key step for synthesis of styrylbenzenes is the Wittig reaction between aldehyde **1**[35] (prepared from 5-formylsalicylic acid) and triphenyl phosphonium salt, **2**[36] or bis(diethyl phosphonate), **3** (Scheme 1). Both Wittig reagents, **2** and **3,** were readily prepared from 2-bromo-*p*-xylene. When the triphenylphosphonium salt, **2**, was used for the Wittig reaction, all four possible isomers [(*E*,*E*)-**4**, (*Z*,*Z*)-**4**, (*E*,*Z*)-**4**, and (*Z*,*E*)-**4**] were formed, of which (*E*,*E*)-**4**, the *trans-trans* isomer, precipitated from the reaction mixture in 11% yield. Alternatively, when bis(diethyl phosphonate), **3**, was used instead of the triphenylphosphonium salt, **2**, for the Wittig−Horner reaction, (*E*,*E*)-**4** was obtained as the sole product in 45% yield, and no other isomers were detected from the reaction mixture (Scheme 1). The selectivity of producing only the *trans* (*E*) isomer of stilbenes by using dialkyl phosphonates has been reported previously.[37] However, for this particular series of styrylbenzenes, the chemical synthesis via a Wittig reaction producing only the *trans-trans* (*E*,*E*) isomer by using bis(diethyl phosphonate) has not been reported. The later procedure using bis(diethyl phosphonate), **3**, not only increased the yield of the *trans-trans* isomer but also eliminated the time-consuming chromatographic purification. Therefore, it is the method of choice to prepare the starting compound (*E*,*E*)-**4**. All of the subsequent styrylbenzenes are in the *trans-trans* (*E*,*E*) form; therefore, the (*E*,*E*) designation is discontinued for all of the other compounds.

Compound **4** was readily converted to **6** (BSB) in two steps: demethylation with BBr_3 in CH_2Cl_2 and hydroly-

Scheme 1

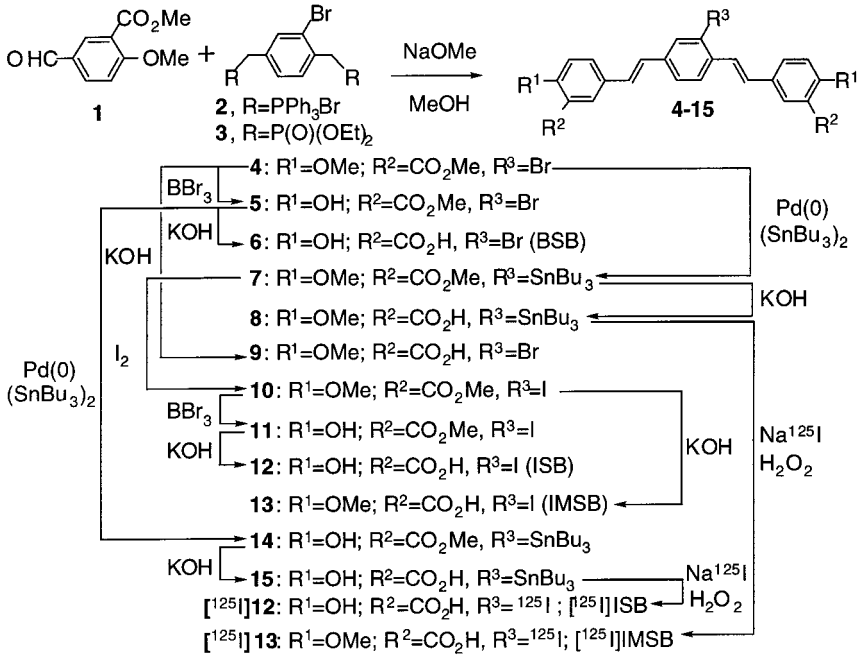

Scheme 2

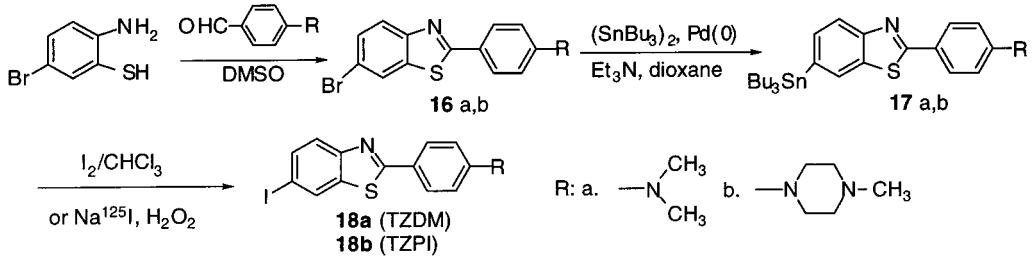

sis of the methyl esters in KOH and EtOH. The methoxy/acid derivative **9** was obtained by hydrolysis of **4** by KOH and EtOH. When **4** was reacted with bis-(tributyltin) using Pd(0) as the catalyst, the corresponding tributyltin derivative **7** was obtained (21% yield). The tributyltin derivative **7** was reacted with iodine in chloroform at room temperature to give the iodo derivative **10** in 87% yield. Hydrolysis of **10** in KOH and EtOH produced **13** (IMSB) in good yield (84%). The methyl groups of the phenolic ether on **10** were readily removed by reacting with BBr_3 to give **11**. Subsequently, **11** was converted to **12** (ISB) using the same base-catalyzed hydrolysis. The other tributyltin derivative **14** was prepared from the corresponding bromo compound **5**, by use of a bromo to tributyltin exchange reaction catalyzed by Pd(0) (25% yield). Hydrolysis of the ester groups of **14** was again achieved in KOH and EtOH to afford **15** in 95% yield (Scheme 1). It is important to note that the tributyltin derivatives (**7**, **8**, **14**, and **15**) are generally sensitive to strong acid-catalyzed decomposition; therefore, it is preferable to prepare the tributyltin derivatives after demethylation in which the acidic BBr_3 was used (e.g., **14** and **15**). The methyl ester groups of **7** and **14** were removed by a base (KOH)-catalyzed hydrolysis, which led to the desired compounds, **8** and **15**. The tributyltin derivatives **8** and **15** can be readily used as the starting materials for radioiodination in preparation of [^{125}I]**12** (ISB) and [^{125}I]-**13** (IMSB).

Preparation of benzothiazole derivatives was achieved by reactions described in Scheme 2. Heating 5-bromo-2-aminobenzenethiol[38,39] and 4-(dimethylamino)benzaldehyde or 4-(4-methylpiperazin-1-yl)benzaldehyde[40] in DMSO produced benzothiazoles, **16a** and **16b**. Using the same Pd(0)-catalyzed bromo to tributyltin exchange reaction, these two bromo derivatives were successfully converted to the corresponding tributyltin derivatives, **17a** and **17b**. They were successfully used in an iodo-destannylation reaction to produce the corresponding iodinated compounds, **18a** and **18b** (yields were between 25 and 35%; the reactions were not optimized). Thus, the tributyltin derivatives served two useful purposes. (i) They served as intermediates for converting bromo to iodo derivatives, and (ii) they are also useful as starting material for preparation of radioiodinated "hot" ligands.

Radiolabeling. The novel radioiodinated ligands, [^{125}I]**12** (ISB), [^{125}I]**13** (IMSB), [^{125}I]**18a** (TZDM), and [^{125}I]**18b** (TZPI), were successfully prepared from the corresponding tributyltin derivatives by an iododestannylation reaction, which resulted in no-carrier-added tracers (specific activity comparable to that of Na^{125}I, 2200 Ci/mmol). The radiochemical identities of the radioiodinated ligands were verified by co-injection with the nonradioactive compounds by their HPLC profiles. All of the radioiodinated ligands displayed excellent in vitro stability for up to 2 months (>95% radiochemically pure as determined by HPLC).

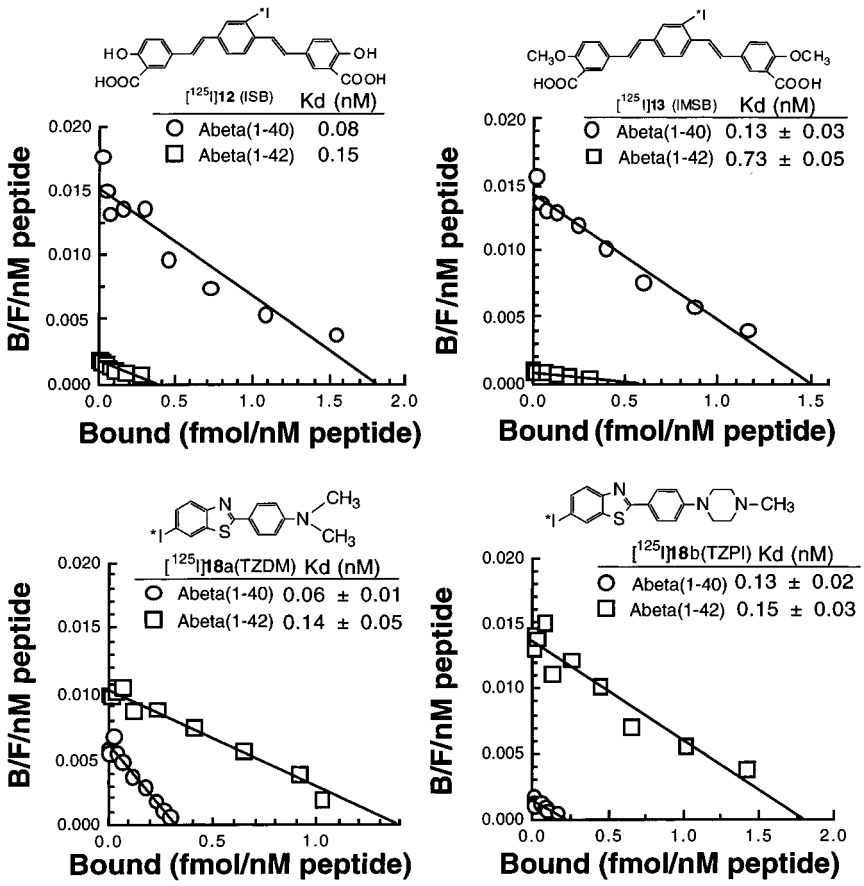

Figure 2. Scatchard plots of four ligands, [^{125}I]**12** (ISB), [^{125}I]**13** (IMSB), [^{125}I]**18a** (TZDM), and [^{125}I]**18b** (TZPI), binding to aggregates of Aβ(1−40) and Aβ(1−42) peptides showing very high affinity. Under the assaying condition, both of the styrylbenzenes, [^{125}I]**12** and [^{125}I]**13**, detected about 2−3-fold more binding sites (B_{max} values in femtomoles per nanomolar peptide as indicated by the intercept on the *x*-axis) on Aβ(1−40) aggregates than on Aβ(1−42) aggregates, while the binding preference of thiazoles, [^{125}I]**18a** and [^{125}I]**18b**, displayed binding for both.

Binding to Aβ Aggregates of Aβ(1−40) and Aβ(1−42). Using these four radioiodinated probes with high specific activity, studies of the binding of the ligands to aggregates of Aβ(1−40) and Aβ(1−42) peptides in solution were carried out. All of the ligands displayed a saturable binding. Transformation of the saturation binding of all of the new ligands to Scatchard plots gave linear plots suggesting one-site binding. The K_d values estimated for [^{125}I]**12**, [^{125}I]**13**, [^{125}I]**18a**, and [^{125}I]**18b** were 0.08, 0.13, 0.06, and 0.13 nM for aggregates of Aβ(1−40) and 0.15, 0.73, 0.14, and 0.15 nM for aggregates of Aβ(1−42), respectively (Figure 2). More importantly, under the assaying conditions, both of the styrylbenzenes, [^{125}I]**12** and [^{125}I]**13**, detected about 2−3-fold more binding sites (B_{max} values in femtomoles per nanomolar peptide as indicated by the intercept on the *x*-axis) on Aβ(1−40) aggregates than on Aβ(1−42) aggregates, while benzothiazoles, [^{125}I]**18a** and [^{125}I]**18b**, displayed an opposite preference, showing 4−5-fold more binding sites on Aβ(1−42) aggregates than on Aβ(1−40) aggregates (Figure 2).

Interestingly, when styrylbenzene derivatives, i.e., CG and IMSB, were evaluated for their competition against [^{125}I]**18a** (a benzothiazole derivative) binding on Aβ(1−40) and Aβ(1−42) aggregates, high K_i values were observed (see Table 1), indicating poor binding competition. Similarly, high K_i values were obtained for **16a** and **16b**, and **18a** and **18b** (benzothiazole derivatives), against binding of [^{125}I]**13** (a styrylbenzene derivative) (Table 1). In comparison, K_i values on competition of CG and IMSB against [^{125}I]**13**, as well as those for benzothiazoles (i.e., **16a**, **16b**, **18a**, and **18b**) against [^{125}I]**18a**, displayed the expected and consistent potencies on both Aβ(1−40) and Aβ(1−42) aggregates. These K_i values presented in Table 1 provide compelling evidence that there are distinctive and mutually exclusive binding sites on Aβ(1−40) and Aβ(1−42) aggregates for these two series of compounds.

Table 1. Inhibition Constants (K_i, nM) of Compounds on Ligand Binding to Aggregates of Aβ(1−40) and Aβ(1−42) at 25 °C[a]

	aggregates of Aβ(1−40)		aggregates of Aβ(1−42)	
compound	vs [^{125}I]**13** (IMSB)	vs [^{125}I]**18a**	vs [^{125}I]**13** (IMSB)	vs [^{125}I]**18a**
chrysamine G	0.14 ± 0.04	>1000	0.4 ± 0.1	>2000
13 (IMSB)	0.17 ± 0.03	>1000	0.8 ± 0.2	>1000
thioflavin T	>9000	116 ± 20	>4000	294 ± 40
16a	>2000	1.9 ± 0.3	>3000	0.8 ± 0.3
16b	>2000	1.6 ± 0.5	>2400	5.0 ± 0.8
18a	>2000	0.9 ± 0.2	>5000	2.2 ± 0.4
18b	>2000	5.4 ± 0.7	>2000	6.4 ± 0.7

[a] Values are means ± standard error of the mean of three independent experiments, each in duplicate.

The unique selectivity demonstrated by these two sets of ligands based on structurally divergent compounds (styrylbenzenes and benzothiazoles) is very striking. To our knowledge, this is the first time such small molecule probes demonstrated specific binding at a sub-nanomo-

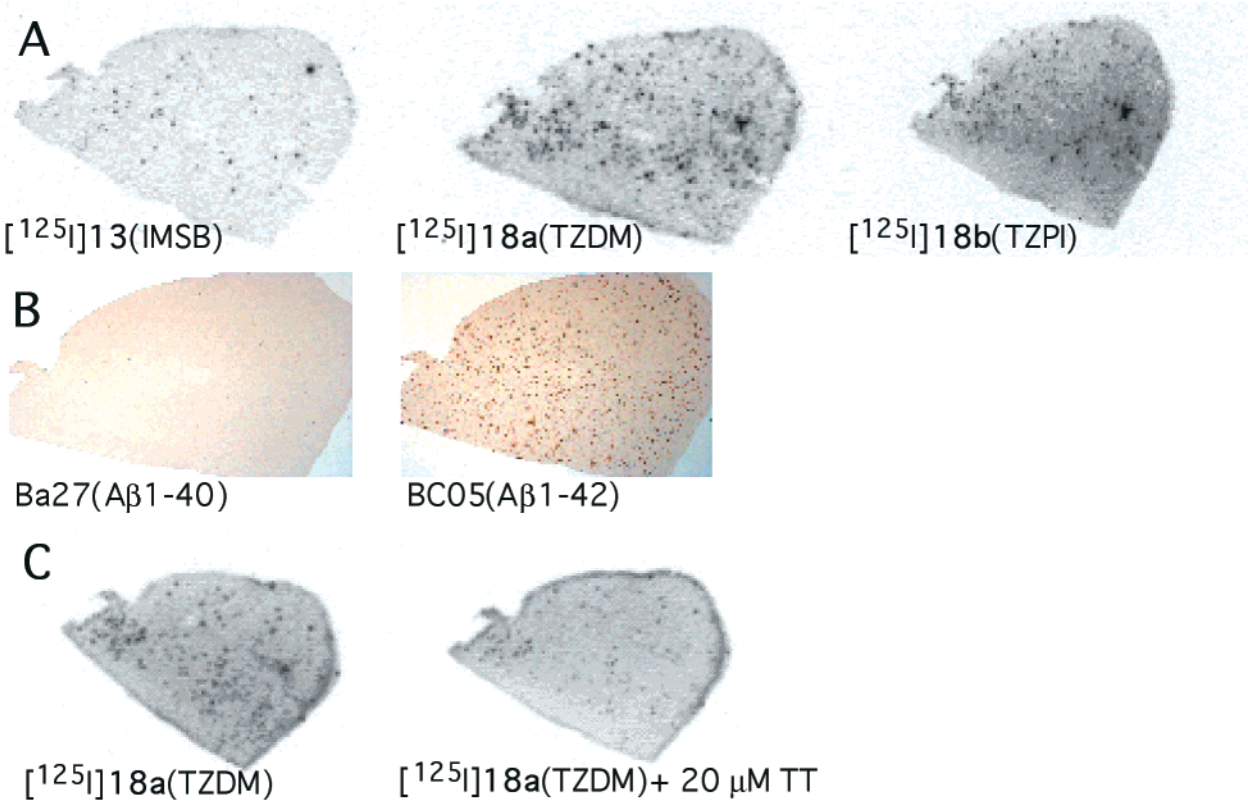

Figure 3. (A) Film autoradiography showing binding of [^{125}I]**13** (IMSB), [^{125}I]**18a** (TZDM), and [^{125}I]**18b** (TZPI) to amyloid plaques of the formalin-fixed brain sections of a Down's syndrome patient containing mainly Aβ(1−42) aggregates. The plaque labeling was clearly visualized in the brain sections labeled with [^{125}I]**18a** (TZDM) and [^{125}I]**18b** (TZPI), both of which primarily label Aβ(1−42) aggregates, while an adjacent section labeled with [^{125}I]**13** (IMSB) showed very little labeling, because IMSB is more selective toward Aβ(1−40) aggregates. (B) Comparable brain sections of the same subject were immunostained by antibodies specific for Aβ(1−40) (Ba27) and Aβ(1−42) (BC05). The autoradiography images of [^{125}I]**18a** (TZDM) and [^{125}I]**18b** (TZPI) displayed high concentrations of Aβ(1−42) aggregates in the brain section, consistent with the high concentration of Aβ(1−42) shown by the immunostaining. (C) The level of plaque labeling of [^{125}I]**18a** (TZDM) was significantly reduced in the presence of 20 μM thioflavin T (TT), indicating TZDM competes with TT for the same binding sites.

lar concentration to Aβ(1−40) and Aβ(1−42) aggregates. It is known that when Aβ(1−40) and Aβ(1−42) peptides are aggregated, they assemble into a fibrillary coil containing β-sheet structures. It is evident that under the conditions used in this study Aβ(1−40) and Aβ(1−42) peptides form aggregates containing two different binding pockets for styrylbenzenes and benzothiazoles (thioflavins). Clearly, there are significant structural differences between these two aggregates, and at least two different binding pockets, possibly more, exist on these aggregates.[41,42] No detailed structural information is currently available on the potential binding sites, nor do we know the full extent of functional linkages of these styrylbenzene or benzothiazole binding sites on Aβ aggregates. It has been suggested previously that binding of small molecules to the Aβ aggregates may prevent further aggregation and reduce their toxicity.[11,41−46] There are still many unanswered questions. Are there any other specific sites with structural requirements which differ from those of styrylbenzene and benzothiazole? Are these sites just "incidental inventions of Mother Nature"? Further testing is warranted to investigate any functional or physiological roles of these binding sites in amyloid plaque (aggregates) formation and cellular toxicity. As such, the feasibility of using these ligands with high binding affinity as potential drugs for treatment of AD can be explored.

The radioiodinated probes, [^{125}I]**13** (IMSB) and [^{125}I]-**18a** (TZDM), may allow the use of high-throughput screening for rapidly selecting agents with the requisite binding affinity (at sub-nanomolar concentrations) and selectivity for aggregated amyloid peptides in solution. Indeed, this strategy may serve as the initial screen for the selection of compounds with the potential to bind to amyloid plaques in vivo.

Labeling of Aβ Aggregates in Human Brain Sections with Radioiodinated Ligands. Since the in vitro binding assays demonstrated the selectivity of the radioiodinated probes for aggregates composed of synthetic Aβ(1−40) and Aβ(1−42) peptides, we asked if these probes showed similar selectivity to Aβ aggregates found in the human brain. To test this, we performed autoradiography using tissue sections from a postmortem Down's syndrome brain. We chose to use the Down's syndrome brain since patients with Down's syndrome invariably develop neuropathological changes characteristic of AD, and these changes begin with the deposition of SPs containing predominantly Aβ(1−42)[47,48] (Figure 3). The sections were immunostained with antibodies Ba27 and BC05 specific for Aβ(1−40) and Aβ(1−42), respectively. It is apparent that [^{125}I]**13** (IMSB) displayed only weak binding to these plaques (Figure 3) with only a few spots of plaque signals, but no intense labeling. This is consistent with the fact that

Table 2. Biodistribution in Mice after iv Injection of ^{125}I-Labeled Styrylbenzenes (**12** or **13**) or ^{125}I-Labeled Thioflavins (**18a** or **18b**) and the Partition Coefficients (PC) of the Ligands[a]

organ	5 min	30 min	60 min
	[^{125}I]**12** (ISB) (PC = 35)		
blood	7.57 ± 1.23	2.98 ± 0.34	2.59 ± 0.18
heart	0.33 ± 0.06	0.17 ± 0.02	0.13 ± 0.03
muscle	5.68 ± 0.79	3.90 ± 0.66	2.98 ± 0.25
lung	0.81 ± 0.12	0.30 ± 0.03	0.25 ± 0.01
kidney	1.67 ± 0.42	0.77 ± 0.05	0.63 ± 0.17
spleen	0.25 ± 0.10	0.13 ± 0.01	0.07 ± 0.01
liver	42.68 ± 2.50	30.16 ± 4.24	19.12 ± 3.11
skin	4.02 ± 0.17	4.13 ± 0.44	3.66 ± 0.29
brain	0.27 ± 0.04	0.06 ± 0.01	0.04 ± 0.01
	[^{125}I]**13** (IMSB) (PC = 1.1)		
blood	22.52 ± 6.03	5.19 ± 1.01	2.17 ± 0.69
heart	0.43 ± 0.11	0.18 ± 0.04	0.12 ± 0.04
muscle	3.16 ± 1.37	1.82 ± 0.28	1.30 ± 0.45
lung	0.89 ± 0.18	0.31 ± 0.08	0.16 ± 0.05
kidney	1.31 ± 0.25	0.46 ± 0.09	0.23 ± 0.05
spleen	0.17 ± 0.02	0.07 ± 0.03	0.03 ± 0.01
liver	47.85 ± 4.61	24.47 ± 4.30	6.14 ± 2.67
skin	1.56 ± 0.63	1.44 ± 0.36	1.02 ± 0.34
brain	0.14 ± 0.03	0.03 ± 0.00	0.02 ± 0.01

organ	2 min	30 min	60 min	6 h	24 h
		[^{125}I]**18a** (TZDM) (PC = 70)			
blood	15.74 ± 6.06	3.26 ± 0.05	3.79 ± 0.19	1.44 ± 0.05	0.29 ± 0.09
heart	1.79 ± 0.39	0.20 ± 0.01	0.17 ± 0.02	0.05 ± 0.01	0.01 ± 0.00
muscle	17.81 ± 2.29	12.89 ± 1.06	12.81 ± 2.78	2.93 ± 0.02	0.33 ± 0.08
lung	5.91 ± 1.39	0.72 ± 0.16	0.78 ± 0.07	0.21 ± 0.04	0.03 ± 0.01
kidney	5.42 ± 0.57	2.24 ± 0.98	2.23 ± 0.41	0.54 ± 0.12	0.06 ± 0.00
spleen	0.59 ± 0.04	0.20 ± 0.05	0.17 ± 0.06	0.04 ± 0.00	0.01 ± 0.00
liver	31.62 ± 2.38	10.93 ± 2.34	9.21 ± 3.05	1.52 ± 0.30	0.3 ± 0.07
skin	3.2 ± 0.45	7.4 ± 0.60	12.8 ± 1.13	3.8 ± 0.07	0.2 ± 0.07
brain	0.6 ± 0.11	0.9 ± 0.29	1.57 ± 0.24	0.65 ± 0.11	0.04 ± 0.01
		[^{125}I]**18b** (TZPI) (PC = 312)			
blood	8.02 ± 0.82	5.15 ± 0.23	4.16 ± 0.28	1.49 ± 0.26	0.41 ± 0.09
heart	2.19 ± 0.43	0.69 ± 0.02	0.66 ± 0.06	0.22 ± 0.06	0.08 ± 0.01
muscle	13.24 ± 3.08	18.82 ± 1.16	19.46 ± 0.30	6.65 ± 0.67	2.44 ± 0.37
lung	12.80 ± 1.54	4.14 ± 0.41	3.38 ± 0.33	1.15 ± 0.31	0.44 ± 0.06
kidney	6.46 ± 1.80	8.06 ± 1.26	7.99 ± 1.45	3.62 ± 0.12	1.15 ± 0.22
spleen	0.89 ± 0.14	0.87 ± 0.22	0.60 ± 0.06	0.22 ± 0.08	0.08 ± 0.01
liver	28.84 ± 3.77	21.22 ± 5.86	17.20 ± 2.49	5.79 ± 1.24	3.05 ± 0.87
skin	4.06 ± 0.52	6.07 ± 0.43	5.63 ± 0.67	3.17 ± 0.27	1.64 ± 0.47
brain	1.50 ± 0.10	1.59 ± 0.19	1.89 ± 0.43	1.08 ± 0.08	0.91 ± 0.08

[a] The % dose/organ; average of three or four mice ± standard deviation.

this section contained only a very small number of Aβ-(1−40) positive plaques [as confirmed by staining with an Aβ(1−40) specific monoclonal antibody, Ba27], and [^{125}I]**13** (IMSB) labels the Aβ(1−40) aggregates preferentially. The level of nonspecific binding observed with [^{125}I]**12** (ISB) was relatively high; therefore, it was not used for this part of the experiment. The distinctive labeling of the plaques by [^{125}I]**18a** (TZDM) and [^{125}I]-**18b** (TZPI) resulted in an excellent autoradiographic visualization of the amyloid plaques [mainly Aβ(1−42) aggregates, stained positively by BC05] in the sections from this patient (Figure 3). The results are consistent with the in vitro observation that these benzothiazoles bind to Aβ(1−42) aggregates with a high affinity.

Biodistribution of New Ligands in Normal Mice. One of the key prerequisites for an in vivo imaging agent of the brain is the ability to cross the intact blood−brain barrier after a bolus iv injection. The lipophilicities of [^{125}I]**12** (ISB) and [^{125}I]**13** (IMSB) were 35 and 1.1, respectively (measured by a partition between 1-octanol and pH 7.4 phosphate buffer). It is interesting to note that the [^{125}I]ISB exhibited a higher partition coefficient as compared to [^{125}I]**13** (IMSB), which has two more methyl groups. This is likely due to the presence of intramolecular hydrogen bonding between the OH group of phenol and the carboxylic group of [^{125}I]**12** (ISB). Intramolecular hydrogen bonding of similar structures has been previously reported.[49]

To test the permeability through the intact blood−brain barrier, these new agents were injected into normal mice. The brain uptake 5 min post iv injection showed relatively low values (0.27 and 0.14% dose/organ for [^{125}I]**12** and [^{125}I]**13**, respectively). The blood level 5 min post iv injection was relatively high, which is very unfavorable (Table 2). For a brain perfusion tracer, the uptake in the rat brain at 2 min after a bolus iv injection is expected to be 2−3% dose/organ (to be useful as potential imaging agents of the brain, the minimum brain uptake will be 0.5% dose/organ). The brain retention level of [^{125}I]**12** and [^{125}I]**13** at later time points was low. The results suggest that these two styrylbenzenes showed relatively low initial permeability on crossing the blood−brain barrier. The potential usefulness of these agents for in vivo imaging after a bolus iv injection appears to be limited.

Two new compounds derived from benzothiazole were prepared to improve the brain uptake after an iv injection. These new compounds are derivatives of

thioflavins, but contain no quaternary ammonium ion; therefore, they are relatively small in size, neutral, and lipophilic (PC = 70 and 312 for [^{125}I]**18a** and [^{125}I]**18b**, respectively). Initial brain uptake of [^{125}I]**18a** and [^{125}I]-**18b** in mice after an iv injection was 0.67 and 1.50% dose/organ, respectively. The brain uptake peaked at 60 min for both compounds with a maximum brain uptake of 1.57 and 1.89% dose/organ, respectively. The blood levels are relatively low throughout the time course that was evaluated. For this series of ligands, the level of specific uptake in the brain is relatively high and the retention in the brain is long. The new thioflavins may provide better candidates for further development of the in vivo imaging agents critically important for evaluation of Alzheimer's disease. A more detailed biodistribution study using transgenic mice containing an excess amount of Aβ aggregate deposition in the brain is currently under way. The preliminary results of such a study appear to further confirm the utility of these new agents. The data will be published elsewhere soon.

Development of Aβ aggregate specific tracers may lead to simple and effective tools for the early and accurate diagnosis of AD as well as for monitoring the progression of this disorder in patients.[6,50] SPECT imaging may also provide a simple technique for studying the efficacy of drugs designed to retard or reverse the formation of fibrillar Aβ aggregates in AD patients. Currently, there is no specific imaging agent available for direct mapping of fibrillar Aβ aggregates in vivo. Given the highly pressing needs for such agents, the timely development of imaging agents for monitoring the burden of senile plaques in vivo is widely regarded by basic and clinical investigators as one of the highest priorities for AD research.[50] We have demonstrated a proof of concept that development of small molecule-based tracers showing a high level of selective binding to the Aβ aggregates in the brain may be feasible.

In conclusion, four novel ligands, [^{125}I]**12** (ISB), [^{125}I]-**13** (IMSB), [^{125}I]**18a** (TZDM), and [^{125}I]**18b** (TZPI), were developed. They may be useful as biomarkers for studies of Aβ(1−40) as well as Aβ(1−42) aggregates for detecting amyloid aggregates in the brain by in vivo and in vitro techniques.

Experimental Section

Reagents used in syntheses were purchased from Aldrich Co. or Fluka Co., and were used without further purification unless otherwise indicated. Anhydrous Na_2SO_4 was used as a drying agent. ^{1}H NMR spectra were obtained on Bruker spectrometers (Bruker DPX 200 and AMX500). Chemical shifts are reported as δ values (parts per million) relative to internal TMS. Coupling constants are reported in hertz. The multiplicity is defined by s (singlet), d (doublet), t (triplet), br (broad), and m (multiplet). Mass spectrometry was performed by the Mass Spectrometry Center, Department of Chemistry, University of Pennsylvania. Elementary analysis was performed by the Analysis Laboratory, Department of Chemistry, University of Pennsylvania.

2-Bromo-1,4-bis(diethylphosphonato)xylene (3). A mixture of 1-bromo-2,5-bis(bromomethyl)benzene[36] (3.43 g, 10 mmol) and triethyl phosphite (3.32 g, 20 mmol) was stirred at 160 °C for 4 h. After the mixture was cooled to room temperature, the mixture was treated under reduced pressure to remove the low-boiling point material and the residue was subjected to flash chromatography (95:5 CH_2Cl_2/MeOH mixture) and gave 4.2 g of **3** (92%). ^{1}H NMR (200 MHz, $CDCl_3$): δ 1.26 (m, 12H), 3.17 (d, J = 20.6 Hz, 2H), 3.36 (d, J = 20.9 Hz, 2H), 3.95−4.14 (m, 8H), 7.20 (d, J = 7.9 Hz, 1H), 7.40 (d, d, J = 2.0, 7.9 Hz, 1H), 7.50 (s, 1H).

1-Bromo-2,5-bis(3-methoxycarbonyl-4-methoxy)styrylbenzene (4). (1) Method A. To a mixture of **1** (1.16 g, 6.0 mmol) and **2** (2.6 g, 3.0 mmol) in MeOH (12 mL) was added a solution of sodium methoxide (1.3 mL, 25 wt % in MeOH) dropwise at 0 °C in an ice bath. The mixture was stirred at room temperature overnight. The solid that formed was filtered and washed with methanol to give (*E*,*E*)-**4** (175 mg, 10.9%).

(2) Method B. To a mixture of **1** (2.7 g, 13.9 mmol) and **3** (3.2 g, 7.0 mmol) in MeOH (20 mL) was added a solution of sodium methoxide (5 mL, 25 wt % in MeOH) dropwise at 0 °C in an ice bath. The mixture was stirred under reflux overnight. The precipitate was collected by filtration and washed with methanol to give (*E*,*E*)-**4** (1.67 g, 44.5%). ^{1}H NMR (500 MHz, $CDCl_3$): δ 3.907 (s, 3H, CH_3O), 3.909 (s, 3H), 3.915 (s, 3H), 3.919 (s, 3H), 6.91 (d, J = 16.3 Hz, 1H), 6.97 (d, J = 8.5 Hz, 1H), 6.98 (d, J = 8.5 Hz, 1H), 6.99 (d, J = 16.4 Hz, 1H), 7.03 (d, J = 16.3 Hz, 1H), 7.34 (d, J = 6.2 Hz, 1H), 7.40 (d, J = 8.2 Hz, 1H), 7.59 (d, d, J = 8.5, 2.1 Hz, 1H), 7.60 (d, J = 8.3 Hz, 1H), 7.65 (d, d, J = 8.7, 2.2 Hz, 1H), 7.69 (s, 1H), 7.94 (s, 1H), 7.95 (s, 1H). MS: *m*/*z* 559 (MNa^+). HRMS: *m*/*z* calcd for $C_{28}H_{26}BrO_6$ (MH^+) 537.0913, found 537.0963.

1-Bromo-2,5-bis(3-methoxycarbonyl-4-hydroxy)styrylbenzene (5). To a solution of (*E*,*E*)-**4** (730 mg, 1.36 mmol) in CH_2Cl_2 (250 mL) was added BBr_3 (10.5 mL, 1 M in hexane) dropwise at −78 °C in a dry ice/acetone bath. The mixture was allowed to warm to room temperature. Water was added, while the reaction mixture was cooled at 0 °C in an ice bath. The mixture was extracted with CH_2Cl_2. The organic phase was dried and filtered. The filtrate was concentrated to afford 636 mg of **5** (92%). The analytical sample was obtained by preparative thin-layer chromatography (PTLC) (1:3 EtOAc/hexane mixture). ^{1}H NMR (200 MHz, $CDCl_3$): δ 3.99 (s, 6H), 6.99 (d, J = 16.3 Hz, 1H), 6.98 (d, J = 16.5 Hz, 1H), 7.01 (d, d, J = 8.3, 2.6 Hz, 2H), 7.04 (d, J = 16.3 Hz, 1H), 7.33 (d, J = 16.5 Hz, 1H), 7.40 (d, J = 8.7 Hz, 1H), 7.60−7.73 (m, 4H), 7.97 (s, 2H), 10.81 (s, 1H), 10.83 (s, 1H). MS: *m*/*z* 509 (MH^+).

1-Bromo-2,5-bis(3-hydroxycarbonyl-4-hydroxy)styrylbenzene (6) (BSB). To a solution of **5** (534 mg, 1.0 mmol) in EtOH (60 mL) was added KOH (1.2 g) in a solid form. The mixture was stirred under reflux for 5 h. The cold mixture was acidified with HCl (10% solution) and extracted with a mixed solvent (9:1 CH_2Cl_2/MeOH mixture). The organic phase was dried and filtered. The filtrate was concentrated to give 480 mg of **6** (BSB) (95%). An analytical sample was obtained by PTLC (9:1:0.05 CH_2Cl_2/MeOH/HOAc mixture). ^{1}H NMR (200 MHz, MeOD): δ 6.96 (d, d, J = 3.4, 8.7 Hz, 2H), 6.99 (d, J = 16.3 Hz, 1H), 7.12 (d, J = 16.3 Hz, 1H), 7.17 (d, J = 16.3 Hz, 1H), 7.34 (d, J = 16.3 Hz, 1H), 7.56 (d, J = 8.4 Hz, 1H), 7.73−7.80 (m, 4H), 8.02 (t, J = 2.6 Hz, 2H). MS: *m*/*z* 480 (M^+). Anal. $C_{24}H_{17}BrO_6 \cdot 0.5H_2O$: C, H.

1-(Tributylstannyl)-2,5-bis(3-methoxycarbonyl-4-methoxy)styrylbenzene (7). A mixture of **4** (200 mg, 0.37 mmol), bis(tributyltin) (0.4 mL), and $Pd(Ph_3P)_4$ (30 mg) in a mixed solvent (20 mL, 3:1 dioxane/triethylamine mixture) was stirred at 90 °C overnight. The solvent was removed, and the residue was purified by PTLC (2:1 hexane/EtOAc mixture) to give 57 mg of product (21%). ^{1}H NMR (200 MHz, $CDCl_3$): δ 0.92 (t, J = 7.1 Hz, 9H), 1.20−1.45 (m, 12H), 1.55−1.68 (m, 6H),3.94 (s, 12H), 6.90−7.08 (m, 6H), 7.40−7.70 (m, 5H), 7.95 (d, J = 2.2 Hz, 1H), 7.98 (d, J = 2.2 Hz, 1H).HRMS: *m*/*z* Calcd for $C_{40}H_{52}SnO_6Na$ (MNa^+): 771.2683; Found: 771.2686.

1-(Tributylstannyl)-2,5-bis(3-hydroxycarbonyl-4-methoxy)styrylbenzene (8). The same reaction as described above for preparing **6** was employed, and **8** was obtained in 78% yield from **7**. ^{1}H NMR (200 MHz, $CDCl_3$): δ 0.93 (t, J = 7.1 Hz, 9H), 1.06−1.40 (m, 12H), 1.52−1.68 (m, 6H), 3.92 (s, 6H), 6.93−7.03 (m, 6H), 7.45−7.68 (m, 6H), 7.97 (m, 1H), 8.03 (m, 1H). HRMS: *m*/*z* calcd for $C_{38}H_{48}O_6SnNa$ (MNa^+) 743.2371, found 743.2370.

1-Bromo-2,5-bis(3-hydroxycarbonyl-4-methoxy)styrylbenzene (9). The same reaction as described above to prepare

6 was employed, and **9** was obtained in 71% yield from **4**. ^{1}H NMR (200 MHz, DMSO-d_6): δ 3.83 (s, 6H), 7.12 (d, d, J = 7.7, 3.2 Hz, 1H), 7.13 (d, J = 16.7 Hz, 2H), 7.27 (s, 1H), 7.34 (d, J = 16.7 Hz, 2H), 7.61 (d, J = 8.1 Hz, 1H), 7.74 (d, J = 8.7 Hz, 2H), 7.86 (br, 4H). HRMS: m/z calcd for $C_{26}H_{22}BrO_6$ (MH^+) 509.0600, found 509.0635. Anal. $C_{26}H_{21}BrO_6$: C, H.

1-Iodo-2,5-bis(3-methoxycarbonyl-4-methoxy)styrylbenzene (10). To a solution of **7** (50 mg, 0.07 mmol) in $CHCl_3$ (20 mL) was added a solution of iodine in $CHCl_3$ (0.5 mL, 1 M) at room temperature. The mixture was stirred at room temperature for 1 h. The $NaHSO_3$ solution (3 mL, 5% in water) and KF (3 mL, 1 M in MeOH) were added successively. The mixture was stirred for 5 min, and the organic phase was separated. The aqueous phase was extracted with CH_2Cl_2, and the combined organic phase was dried over Na_2SO_4, filtered, and concentrated to give the crude product. PTLC (2:1 hexane/EtOAc mixture) gave 34 mg of product (87% yield). ^{1}H NMR (200 MHz, $CDCl_3$): δ 3.93 (s, 12H), 6.84−7.24 (m, 6H), 7.43−7.70 (m, 4H), 7.95 (d, J = 1.4 Hz, 2H), 7.98 (d, J = 1.4 Hz, 1H). HRMS: m/z calcd for $C_{28}H_{25}IO_6Na$ (MNa^+) 607.0594, found 607.0579.

1-Iodo-2,5-bis(3-hydroxycarbonyl-4-hydroxy)styrylbenzene (11). The same reaction as described above to prepare **5** was employed, and **11** was obtained in 75% yield from **10**. ^{1}H NMR (200 MHz, $CDCl_3$): δ 3.99 (s, 6H), 6.81−7.22 (m, 6H), 7.46−7.70 (m, 4H), 7.95 (d, J = 2.0 Hz, 2H), 7.98 (d, J = 1.3 Hz, 1H), 10.80 (s, 1H), 10.83 (s, 1H).

1-Iodo-2,5-bis(3-hydroxycarbonyl-4-hydroxy)styrylbenzene (12). The same reaction as described above to prepare 6 was employed, and **12** was obtained in 83% yield from **11**. ^{1}H NMR (200 MHz, MeOD): δ 6.46−7.23 (m, 6H), 7.49−7.74 (m, 4H), 7.98 (m, 3H). HRMS: m/z calcd for $C_{24}H_{17}IO_6Na$ (MNa^+) 550.9968, found 550.9941. Anal. $C_{24}H_{17}IO_6 \cdot 0.5H_2O$: C, H.

1-Iodo-2,5-bis(3-hydroxycarbonyl-4-methoxy)styrylbenzene (13). The same reaction as described above to prepare **6** was employed, and **13** was obtained in 84% yield from **10**. ^{1}H NMR (200 MHz, $CDCl_3$): δ 10 (s, 6H), 6.88−7.29 (m, 6H), 7.43 (d, J = 8.2 Hz, 1H), 7.55 (d, J = 8.2 Hz, 1H), 7.67 (d, d, J = 9.0, 2.3 Hz, 1H), 7.77 (d, d, J = 9.0, 2.3 Hz, 1H), 7.97 (d, J = 1.4 Hz, 1H), 8.29 (d, J = 1.4 Hz, 1H), 8.30 (d, J = 1.4 Hz, 1H). HRMS: m/z calcd for $C_{26}H_{21}IO_6Na$ (MNa^+) 579.0281, found 579.0292. Anal. $C_{26}H_{21}IO_6$: C, H.

1-(Tributylstannyl)-2,5-bis(3-methoxycarbonyl-4-hydroxy)styrylbenzene (14). The same reaction as described above to prepare **7** was employed, and **14** was obtained in 25% yield from **5**. ^{1}H NMR (200 MHz, $CDCl_3$): δ 0.80 (t, J = 7.2 Hz, 9H), 1.00−1.36 (m, 12H), 1.43−1.62 (m, 6H), 3.92 (s, 6H), 6.85 (d, J = 15.8 Hz, 2H), 6.94 (m, 2H), 6.95 (d, J = 15.8 Hz, 2H), 7.39−7.64 (m, 5H), 7.89 (d, J = 2.1 Hz, 2H), 10.71 (s, 2H).

1-(Tributylstannyl)-2,5-bis(3-hydroxycarbonyl-4-hydroxy)styrylbenzene (15). The same reaction as described above to prepare **6** was employed, and **15** was obtained in 26% yield from **14**. ^{1}H NMR (200 MHz, MeOD): δ 0.86 (t, J = 7.2 Hz, 9H), 1.10−1.40 (m, 12H), 1.45−1.68 (m, 6H), 6.90−7.24 (m, 6H), 7.39−7.72 (m, 5H), 8.01 (s, 2H).

2-[4′-(Dimethylamino)phenyl]-6-bromobenzothiazole[33,34] (16a). A mixture of 5-bromo-2-aminobenzenethiol[38,39] (306 mg, 1.5 mmol) and 4-(dimethylamino)benzaldehyde (224 mg, 1.5 mmol) in DMSO was heated at 180 °C for 15 min. Water (10 mL) was added after the mixture was cooled. The solid was collected by suction and recrystallized in ethyl acetate to give 340 mg of product (68%). ^{1}H NMR (200 MHz, $CDCl_3$): δ 3.06 (s, 6H), 6.74 (d, J = 9.0 Hz, 2H), 7.52 (d, d, J = 8.7, 2.0 Hz, 1H), 7.82 (d, J = 8.6 Hz, 1H), 7.93 (d, J = 8.8 Hz, 2H), 7.95 (s, 1H). HRMS: m/z calcd for $C_{15}H_{14}BrN_2S$ (MH^+) 333.0061, found 333.0072.

2-[4′-(4″-Methylpiperazin-1-yl)phenyl]-6-bromobenzothiazole (16b). The procedure described above to prepare **16a** was employed to give 57.2% of product **16b** from 4-(4-methylpiperazin-1-yl)benzaldehyde[40] (204 mg, 1 mmol) and 5-bromo-2-aminobenzenethiol (204 mg, 1 mmol). ^{1}H NMR (200 MHz, $CDCl_3$): δ 2.38 (s, 3H), 2.60 (t, J = 5.0 Hz, 4H), 3.38 (t, J = 5.0 Hz, 4H), 6.96 (d, J = 8.9 Hz, 2H), 7.54 (d, d, J = 8.5, 1.9 Hz, 1H), 7.83 (d, J = 8.5 Hz, 1H), 7.95 (d, J = 8.9 Hz, 2H), 7.98 (s, 1H). HRMS: m/z calcd for $C_{18}H_{19}BrN_3S$ (MH^+) 388.0483, found 388.0474.

2-[4′-(Dimethylamino)phenyl]-6-(tributylstannyl)benzothiazole (17a). To a solution of 2-[4′-(dimethylamino)-phenyl]-6-bromobenzothiazole (**16a**) (60 mg, 0.18 mmol) in 1,4-dioxane (2 mL), toluene (2 mL), and triethylamine (2 mL) was added $(Bu_3Sn)_2$ (0.2 mL) followed by $Pd(Ph_3P)_4$ (20 mg). The mixture was stirred at 90 °C overnight. The solvent was removed, and the residue was purified by PTLC (6:1 hexane/EtOAc mixture) to give 33 mg of product (33.6% yield). ^{1}H NMR (200 MHz, $CDCl_3$): δ 0.90 (t, J = 7.1 Hz, 9H), 1.10 (t, J = 8.0 Hz, 6H), 1.34 (hex, J = 7.3 Hz, 6H), 1.57 (m, 6H), 3.05 (s, 6H), 6.74 (d, J = 9.0 Hz, 2H), 7.50 (d, d, J = 7.9, 0.9 Hz, 1H), 7.93 (s, 1H), 7.95 (d, J = 8.5 Hz, 1H), 7.97 (d, J = 9.0 Hz, 2H). HRMS: m/z calcd for $C_{27}H_{41}N_2SSn$ (MH^+) 545.2012, found 545.2035.

2-[4′-(4″-Methylpiperazin-1-yl)phenyl]-6-(tributylstannyl)benzothiazole (17b). The procedure described above to prepare **17a** was employed, and **17b** was obtained in 23% yield from **16b**. ^{1}H NMR (200 MHz, $CDCl_3$): δ 0.89 (t, J = 7.2 Hz, 9H), 1.06 (t, J = 8.2 Hz, 6H), 1.30 (hex, J = 7.3 Hz, 6H), 1.57 (pen, J = 7.2 Hz, 6H), 2.38 (s, 3H), 2.60 (m, 4H), 3.36 (t, J = 5.0 Hz, 4H), 6.96 (d, J = 8.9 Hz, 2H), 7.52 (d, J = 7.9 Hz, 1H), 7.93 (s, 1H), 7.95 (d, J = 7.9 Hz, 1H), 7.98 (d, J = 8.9 Hz, 2H). HRMS: m/z calcd for $C_{30}H_{46}N_3SSn$ (MH^+) 600.2434, found 600.2449.

2-[4′-(Dimethylamino)phenyl]-6-iodobenzothiazole (18a, TZDM). To a solution of **17a** (45 mg, 0.08 mmol) in $CHCl_3$ (10 mL) was added a solution of iodine (1 mL, 1 M in $CHCl_3$) dropwise at room temperature until it became dark red. The resulting mixture was stirred at room temperature for 10 min. The $NaHSO_3$ solution (2 mL, 5% in water) and KF (1 mL, 1 M in MeOH) were added successively. The mixture was stirred for 5 min, and the organic phase was separated. The aqueous phase was extracted with CH_2Cl_2, and the combined organic phase was dried over Na_2SO_4, filtered, and concentrated to give the crude product which was purified by PTLC (6:1 hexane/EtOAc) to give 9 mg of the desired product (29% yield). ^{1}H NMR (200 MHz, $CDCl_3$): δ 3.06 (s, 6H), 6.73 (d, J = 9.0 Hz, 2H), 7.69 (s, 1H), 7.70 (s, 1H), 7.93 (d, J = 9.0 Hz, 2H), 8.15 (s, 1H). HRMS: m/z calcd for $C_{15}H_{13}N_2IS$ (MH^+) 380.9922, found 380.9914. Anal. $C_{15}H_{14}N_3IS$: C, H, N.

Under two different HPLC conditions (A and B), **18a** (TZDM) appeared as one single peak that was >95% pure.

System A included a Phenomenex Nucleosil Si, 10 μm, 250 mm × 4.6 mm column, a 3:1 hexane/ethyl acetate mixture as the solvent, a flow rate of 0.8 mL/min, and a retention time of 4.9 min.

System B included a Phenomenex Luna C8, 5 μm, 250 mm × 4.6 mm column, a 9:1 acetonitrile/5 mM 3,3-dimethylglutarate mixture as the solvent (pH 7.0), a flow rate of 1.0 mL/min, and a retention time of 7.1 min.

2-[4′-(4″-Methylpiperazin-1-yl)phenyl]-6-iodobenzothiazole 18b (TZPI). The same reaction as described above to prepare **18a** was employed, and **18b** was obtained in 36% yield from **17b**. ^{1}H NMR (200 MHz, $CDCl_3$): δ 2.42 (s, 3H), 263 (t, J = 4.8 Hz, 4H), 3.40 (t, J = 4.9 Hz, 4H), 6.95 (d, J = 9.0 Hz, 2H), 7.71 (s, 1H), 7.72 (s, 1H), 7.95 (d, J = 8.9 Hz, 2H), 8.17 (t, J = 1.0 Hz, 1H). HRMS: m/z calcd for $C_{18}H_{19}N_3IS$ (MH^+) 436.0344, found 436.0364. Anal. $C_{18}H_{18}N_3SI$: C, H, N.

Preparation of Radioiodinated Ligands. The four desired ^{125}I-labeled compounds were prepared using iododestannylation reactions with tributyltin precursors **8**, **15**, **17a**, and **17b**.[51] Hydrogen peroxide (50 μL, 3% w/v) was added to a mixture of 50 μL of the correspondent tributyltin precursor (1 mg/mL EtOH), 50 μL of 1 N HCl, and $Na^{125}I$ (1−5 μCi) in a closed vial. The reaction was allowed to proceed for 10 min at room temperature and terminated by addition of 100 μL of saturated $NaHSO_3$. The reaction mixture was either directly extracted (styrylbenzenes) with ethyl acetate (3 × 1 mL) or extracted after neutralization with a saturated sodium bicarbonate solution (thioflavins). The combined extracts were

evaporated to dryness. For styrylbenzenes, the residues were dissolved in 100 μL of EtOH and purified by HPLC using a reversed phase column (Waters ubondpad, 3.9 mm × 300 mm) with an isocratic solvent mixture of 65% acetonitrile and 35% trifluoroacetic acid (0.1%) at a flow rate of 0.8 mL/min. Thioflavins were purified on a C4 column (Phenomenex Inc., Torrance, CA) eluted with an isocratic solvent of 80% acetonitrile and 20% 3,3-dimethylglutaric acid (5 mM, pH 7.0) and a flow rate of 0.8 mL/min. The desired fractions containing the product were collected, condensed, and re-extracted with ethyl acetate. The no-carrier-added products were evaporated to dryness and redissolved in 100% EtOH (1 μCi/μL). The final ^{125}I probes, with a specific activity of 2200 Ci/mmol and a radiochemical purity of >95%, were stored at −20 °C for up to 6 weeks for in vitro binding and autoradiography studies.

Partition Coefficient Determination. Partition coefficients were measured by mixing the ^{125}I tracer with 3 g each of 1-octanol and buffer (0.1 M phosphate, pH 7.4) in a test tube. The test tube was vortexed for 3 min at room temperature, followed by centrifugation for 5 min. Two weighed samples (0.5 g each) from the 1-octanol and buffer layers were counted in a well counter. The partition coefficient was determined by calculating the ratio of counts per minute per gram of 1-octanol to that of buffer. Samples from the 1-octanol layer were repartitioned until consistent partitions of coefficient values were obtained. The measurement was carried out in triplicate and repeated three times.

Binding Assays Using the Aggregated Aβ(1−40) or Aβ-(1−42) Peptide in Solution. The solid forms of peptides Aβ-(1−40) and Aβ(1−42) were purchased from Bachem (King of Prussia, PA). Aggregation of peptides was carried out by gently dissolving the peptide [0.5 mg/mL for Aβ(1−40) and 0.25 mg/mL for Aβ (1−42)] in a buffer solution (pH 7.4) containing 10 mM sodium phosphate and 1 mM EDTA. The solutions were incubated at 37 °C for 36−42 h with gentle and constant shaking. Binding studies were carried out in 12 mm × 75 mm borosilicate glass tubes according to the procedure described previously[15] with some modifications. Aggregated fibrils (10−50 nM in the final assay mixture) were added to the mixture containing 50 μL of radioligands (0.01−0.5 nM in 40% EtOH) and 10% EtOH in a final volume of 1 mL for saturation studies. The final concentration of EtOH was 10%. Nonspecific binding was defined in the presence of 800 nM CG for styrylbenzenes or 2 μM thioflavin T for thioflavins. For inhibition studies, 1 mL of the reaction mixture contained 40 μL of inhibitors (10^{-5}−10^{-10} M in 10% EtOH) and 0.05 nM radiotracer in 40% EtOH. The mixture was incubated at room temperature for 3 h, and the bound and free radioactivities were separated by vacuum filtration through Whatman GF/B filters using a Brandel M-24R cell harvester followed by 2 × 3 mL washes of 10% ethanol at room temperature. Filters containing the bound ^{125}I ligand were counted in a γ-counter (Packard 5000) with 70% counting efficiency. Under the assay conditions, the percent of the specifically bound fraction was less than 20% of the total radioactivity. The results of saturation and inhibition experiments were subjected to nonlinear regression analysis using EBDA,[52] by which K_d and K_i values were calculated.

In Vitro Labeling of Brain Sections from a Down's Syndrome Patient by Film Autoradiography. Brain samples from a patient with Down's syndrome were obtained at autopsy, and neuropathological diagnosis was confirmed by current criteria (NIA-Reagan Institute Consensus Group, 1997). Serial sections (6 μm thick) of paraffin-embedded blocks of cortex fixed by immersion in 10% neutral buffered formalin were utilized for staining. Prior to radiolabeling, paraffin sections were taken through two 5 min washes in xylene, followed by 1 min washes sequentially with 100, 100, 95, 85, and 70% EtOH. The sections were blow dried and labeled with 0.3 nM [^{125}I]**13** (IMSB) at room temperature for 3 h and washed with saturated Li_2CO_3 in 40% EtOH for 30 s. Sections labeled with [^{125}I]**18a** or [^{125}I]**18b** were incubated at a ligand concentration between 0.03 and 0.06 nM at room temperature for 1 h. The sections were then washed in 1% acetic acid in 40% EtOH (two 3 min washes) for [^{125}I]**18a**. For [^{125}I]**18b**, the sections were washed with saturated Li_2CO_3 in 40% EtOH for 2 min. All sections were then washed in 40% EtOH for 2 min followed by water for 30 s. After drying, the labeled sections were exposed to Cronex MRF-34 film for 72 h. The films were developed and digitized.

Immunostaining. Sections were deparaffinized in xylene and rehydrated to 70% EtOH and incubated in a methanol/30% H_2O_2 mixture for 30 min before being blocked in a 0.1 M Tris/2% donor horse serum mixture for 5 min. The anti-Abeta monoclonal antibodies Ba27 [selective antibody for Aβ(1−40), Takeda Pharmaceuticals] and BC05 [selective antibody for Aβ-(1−42), Takeda Pharmaceuticals] were applied at a 1:150000 dilution, and slides were incubated at 4 °C overnight. Sections were washed and blocked again in a 0.1 M Tris/2% donor horse serum mixture for 5 min, and biotinylated anti-mouse antibody was applied for 1 h. Sections were washed, and staining was visualized using the avidin−biotin peroxidase kit (Vector-stain ABC kit, Vector Laboratories) and 3,3′-diaminobenzidine tetrahydrochloride.

In Vivo Biodistribution of New Probes in Normal Mice. While under ether anesthesia, 0.15 mL of a saline solution containing labeled agents (5−10 μCi) was injected directly into the tail vein of ICR mice (2−3 months old, average weight of 20−30 g). The mice were sacrificed by cardiac excision at various time points postinjection. The organs of interest were removed and weighed, and the amount of radioactivity was counted with an automatic γ-counter (Packard 5000). The percentage dose per organ was calculated by a comparison of the tissue counts to suitably diluted aliquots of the injected material. Total activities of blood and muscle were calculated under the assumption that they were 7 and 40% of the total body weight, respectively.

Acknowledgment. We thank Ms. Laura Cesaro for her editorial assistance. This work was supported by grants from the National Institutes of Health (NS 18509 to H.F.K. and PO1 AG-11542 to V.M.-Y.L.), the Institute for the Study of Aging (M.-P.K.), and a Medical Scientist Training Program Predoctoral Fellowship from the National Institutes of Health (D.M.S.). We also thank Dr. N. Suzuki and Takeda Pharmaceutical, Inc., for providing the monoclonal antibodies for Aβ(1−40) and Aβ(1−42).

References

(1) Ginsberg, S. D.; Schmidt, M. L.; Crino, P. B.; Eberwine, J. H.; Lee, V. M.-Y.; et al. Molecular pathology of Alzheimer's disease and related disorders. *Cerebral cortex: neurodegenerative and age-related changes in structure and function of cerebral cortex*; Kluwer Academic/Plenum: New York, 1999; pp 603−654.

(2) Selkoe, D. J. Biology of β-amyloid precursor protein and the mechanism of Alzheimer's disease. *Alzheimer's Disease*; Lippincot, Williams & Wilkins: Philadelphia, 1999; pp 293−310.

(3) Vogelsberg-Ragaglia, V.; Trojanowski, J. Q.; Lee, V. M.-Y. Cell biology of tau and cytoskeletal pathology in Alzheimer's disease. *Alzheimer's Disease*; Lippincot, Williams & Wilkins: Philadelphia, 1999; pp 359−372.

(4) Selkoe, D. J. The origins of Alzheimer's disease: A is for amyloid. *J. Am. Med. Assoc.* **2000**, *283*, 1615−1617.

(5) Naslund, J.; Haroutunian, V.; Mohs, R.; Davis, K. L.; Davies, P.; et al. Correlation between elevated levels of amyloid β-peptide in the brain and cognitive decline. *J. Am. Med. Assoc.* **2000**, *283*, 1571−1577.

(6) Golde, T. E.; Eckman, C. B.; Younkin, S. G. Biochemical detection of Aβ isoforms: implications for pathogenesis, diagnosis, and treatment of Alzheimer's disease. *Biochim. Biophys. Acta* **2000**, *1502*, 172−187.

(7) Skovronsky, D. M.; Lee, V. M. β-Secretase revealed: starting gate for race to novel therapies for Alzheimer's disease. *Trends Pharmacol. Sci.* **2000**, *21*, 161−163.

(8) Vassar, R.; Bennett, B. D.; Babu-Khan, S.; Kahn, S.; Mendiaz, E. A.; et al. β-Secretase cleavage of Alzheimer's amyloid precursor protein by the transmembrane aspartic protease BACE. *Science* **1999**, *286*, 735−741.

(9) Wolfe, M. S.; Citron, M.; Diehl, T. S.; Xia, W.; Donkor, I. O.; et al. A substrate-based difluoro ketone selectively inhibits Alzheimer's γ-secretase activity. *J. Med. Chem.* **1998**, *41*, 6−9.

(10) Moore, C. L.; Leatherwood, D. D.; Diehl, T. S.; Selkoe, D. J.; Wolfe, M. S. Difluoro ketone peptidomimetics suggest a large S1 pocket for Alzheimer's γ-secretase: implications for inhibitor design. *J. Med. Chem.* **2000**, *43*, 3434−3442.
(11) Findeis, M. A. Approaches to discovery and characterization of inhibitors of amyloid β-peptide polymerization. *Biochim. Biophys. Acta* **2000**, *1502*, 76−84.
(12) Kuner, P.; Bohrmann, B.; Tjernberg, L. O.; Naslund, J.; Huber, G.; et al. Controlling polymerization of β-amyloid and prion-derived peptides with synthetic small molecule ligands. *J. Biol. Chem.* **2000**, *275*, 1673−1678.
(13) Ashburn, T. T.; Han, H.; McGuinness, B. F.; Lansbury, P. T., Jr. Amyloid probes based on Congo Red distinguish between fibrils comprising different peptides. *Chem. Biol.* **1996**, *3*, 351−358.
(14) Han, G.; Cho, C.-G.; Lansbury, P. T., Jr. Technetium complexes for the quantitation of brain amyloid. *J. Am. Chem. Soc.* **1996**, *118*, 4506−4507.
(15) Klunk, W. E.; Debnath, M. L.; Pettegrew, J. W. Small-molecule β-amyloid probes which distinguish homogenates of Alzheimer's and control brains. *Biol. Psychiatry* **1994**, *35*, 627.
(16) Klunk, W. E.; Debnath, M. L.; Pettegrew, J. W. Chrysamine-G binding to Alzheimer's and control brain: autopsy study of a new amyloid probe. *Neurobiol. Aging* **1995**, *16*, 541−548.
(17) Klunk, W. E.; Hamilton, R. L.; Styren, S. D.; Styren, G.; Debnath, M. L.; et al. Staining of AD and Tg2576 mouse brain with X-34, a highly fluorescent derivative of chrysamine G and a potential in vivo probe for β-sheet fibrils (abstract 636.12). *Soc. Neurosci. Abstr.* **1997**, *23*, 1638.
(18) Mathis, C. A.; Mahmood, K.; Debnath, M. L.; Klunk, W. E. Synthesis of a lipophilic, radioiodinated ligand with high affinity to amyloid protein in Alzheimer's disease brain tissue. *J. Labelled Compd. Radiopharm.* **1997**, *39*, 594−95.
(19) Lorenzo, A.; Yankner, B. A. β-Amyloid neurotoxicity requires fibril formation and is inhibited by congo red. *Proc. Natl. Acad. Sci. U.S.A.* **1994**, *91*, 12243−12247.
(20) Zhen, W.; Han, H.; Anguiano, M.; Lemere, C. A.; Cho, C. G.; et al. Synthesis and amyloid binding properties of rhenium complexes: preliminary progress toward a reagent for SPECT imaging of Alzheimer's disease brain. *J. Med. Chem.* **1999**, *42*, 2805−2815.
(21) Klunk, W. E.; Pettegrew, J. W.; Abraham, D. J. Quantitative evaluation of congo red binding to amyloid-like proteins with a β-pleated sheet conformation. *J. Histochem. Cytochem.* **1989**, *37*, 1273−1281.
(22) Bourguignon, M. H.; Pauwels, E. K. J.; Loc'h, C.; Mazière, B. I-123 Labeled radiopharmaceuticals and single-photon emission tomography: a natural liaison. *Eur. J. Nucl. Med.* **1997**, *24*, 331−334.
(23) Bornebroek, M.; Verzijlbergen, J. F.; Haan, J.; Van Scheyen, E. J.; Verhoeff, N. P.; et al. Potential for imaging cerebral amyloid deposits using [^{123}I]-labelled serum amyloid P component and SPET. *Nucl. Med. Commun.* **1996**, *17*, 929−933.
(24) Saito, Y.; Buciak, J.; Yang, J.; Pardridge, W. M. Vector-mediated delivery of [^{125}I] labeled β-amyloid peptide Aβ1−40 through the blood-brain barrier and binding to Alzheimer's disease amyloid of the Aβ 1−40/vector complex. *Proc. Natl. Acad. Sci. U.S.A.* **1995**, *92*, 10227−10231.
(25) Kabalka, G. W.; Akula, M. R.; Zhang, Z. Y. Regiospecific synthesis of 3,3′-[{2-[^{123}I]iodo-1,1′-biphenyl}-4,4′-diylbis(azo)]bis-[4-amino-1-naphthalenesulfonic acid] disodium salt. *J. Labelled Compd. Radiopharm.* **1997**, *39*, 581.
(26) Dezutter, N. A.; De Groot, T. J.; Busson, R. H.; Janssen, G. A.; Verbruggen, A. M. Preparation of 99mTc−N2S2 conjugates of chrysamine G, potential probes for the β-amyloid protein of Alzheimer's disease. *J. Labelled Compd. Radiopharm.* **1999**, *42*, 309−324.
(27) Dezutter, N. A.; Dom, R. J.; de Groot, T. J.; Bormans, G. M.; Verbruggen, A. M. 99mTc-MAMA-chrysamine G, a probe for β-amyloid protein of Alzheimer's disease. *Eur. J. Nucl. Med.* **1999**, *26*, 1392−1399.
(28) Kurihara, A.; Pardridge, W. M. Aβ(1−40) peptide radiopharmaceuticals for brain amyloid imaging: [^{111}In] chelation, conjugation to poly(ethylene glycol)-biotin linkers, and autoradiography with Alzheimer's disease brain sections. *Bioconjugate Chem.* **2000**, *11*, 380−386.
(29) Wengenack, T. M.; Curran, G. L.; Poduslo, J. F. Targeting Alzheimer's amyloid plaques in vivo. *Nat. Biotechnol.* **2000**, *18*, 868−872.
(30) Styren, S. D.; Hamilton, R. L.; Styren, G. C.; Klunk, W. E. X-34, A Fluorescent Derivative of Congo Red. A novel histochemical stain for Alzheimer's disease pathology. *J. Histochem. Cytochem.* **2000**, *48*, 1223−1232.
(31) Skovronsky, D.; Zhang, B.; Kung, M.-P.; Kung, H. F.; Trojanowski, J. Q.; et al. In vivo detection of amyloid plaques in a mouse model of Alzheimer's disease. *Proc. Natl. Acad. Sci. U.S.A.* **2000**, *97*, 7609−7614.
(32) Elhaddaoui, A.; Pigorsch, E.; Delacourte, A.; Turrell, S. Competition of congo red and thioflavin S binding to amyloid sites in Alzheimer's diseased tissue. *Biospectroscopy* **1995**, *1*, 351−356.
(33) Stevens, M. F. G.; McCall, C. J.; Lelievald, P.; Alexander, P.; Richter, A.; et al. Structural Studies on Bioactive Compounds. Synthesis of Polyhydroxylated 2-Phenylbenzothiazoles and a Comparison of their Cytotoxicities and Pharmacological Properties with Genistein and Quercetin. *J. Med. Chem.* **1994**, *37*, 1689−1695.
(34) Stevens, M. F. G.; McCall, C. J.; Lelieveld, P. (Cancer Research Campaign Technology Ltd.) Benzazole compounds for use in therapy. PCT Int. Appl. WO19940830, 1995; p 47.
(35) Filler, R.; Lin, S.; Zhang, Z. Synthesis of fluorovinylsalicylic acids and their derivatives. *J. Fluorine Chem.* **1995**, *74*, 69−76.
(36) Katz, T. J.; Sudhaka, R. A.; Teasley, M. F.; Gilbert, A. M.; Geiger, W. E.; et al. Synthesis and properties of optically active helical metallocene oligomers. *J. Am. Chem. Soc.* **1993**, *115*, 3182−3198.
(37) Bottin-Strzalko, T.; Seyden-Penne, J. Could *cis*-stilbene be prepared from a benzylic phosphonate by a Wittig−Horner reaction? *Bull. Soc. Chim. Fr.* **1984**, 161−163.
(38) Mital, R. L.; Jain, S. K. Synthesis of some 5-substituted 2-aminobenzenethiols and their conversion into phenothiazines via smiles rearrangement. *J. Chem. Soc.* **1969**, 2148.
(39) Lin, A.-J.; Kasina, S. Synthesis of 3-substituted 7-(3,3-Dimethyl-1-triazeno)-10-methylphenothiazines as potential antitumor agents. *J. Heterocycl. Chem.* **1981**, *18*, 759.
(40) Tanaka, A.; Terasawa, T.; Hagihara, H.; Sakuma, Y.; Ishibe, N.; et al. Inhibitors of Acyl-CoA: cholesterol O-acyltransferase. Identification and structure−activity relationships of a novel series of N-alkyl-N-(heteroaryl-substituted benzyl)-N′-arylureas. *J. Med. Chem.* **1998**, *41*, 2390.
(41) Howlett, D. R.; Perry, A. E.; Godfrey, F.; Swatton, J. E.; Jennings, K. H.; et al. Inhibition of fibril formation in β-amyloid peptide by a novel series of benzofurans. *Biochem. J.* **1999**, *340*, 283−289.
(42) LeVine, H., III; Scholten, J. D. Screening for pharmacologic inhibitors of amyloid fibril formation. *Methods Enzymol.* **1999**, *309*, 467−476.
(43) Klunk, W. E.; Debnath, M. L.; Koros, A. M.; Pettegrew, J. W. Chrysamine-G, a lipophilic analogue of Congo red, inhibits Aβ-induced toxicity in PC12 cells. *Life Sci.* **1998**, *63*, 1807−1814.
(44) Howlett, D. R.; George, A. R.; Owen, D. E.; Ward, R. V.; Markwell, R. E. Common structural features determine the effectiveness of carvedilol, daunomycin and rolitetracycline as inhibitors of Alzheimer's β-amyloid fibril formation. *Biochem. J.* **1999**, *343*, 419−423.
(45) Hughes, E.; Burke, R. M.; Doig, A. J. Inhibition of toxicity in the β-amyloid peptide fragment β-(25−35) using *N*-methylated derivatives: a general strategy to prevent amyloid formation. *J. Biol. Chem.* **2000**, *275*, 25109−25115.
(46) Klunk, W. E.; Jacob, R. F.; Mason, R. P. Quantifying amyloid β-peptide (Aβ) aggregation using the Congo red-Aβ (CR-Aβ) spectrophotometric assay. *Anal. Biochem.* **1999**, *266*, 66−76.
(47) Iwatsubo, T.; Mann, D. M.; Odaka, A.; Suzuki, N.; Ihara, Y. Amyloid β protein (Aβ) deposition: Aβ 42(43) precedes Aβ 40 in Down syndrome. *Ann. Neurol.* **1995**, *37*, 294−299.
(48) Lemere, C. A.; Blusztajn, J. K.; Yamaguchi, H.; Wisniewski, T.; Saido, T. C.; et al. Sequence of deposition of heterogeneous amyloid β-peptides and APO E in Down's syndrome: implications for initial events in amyloid plaque formation. *Neurobiol. Dis.* **1996**, *3*, 16−32.
(49) Denisov, G. S.; Golubev, N. S.; Schreiber, V. M.; Shajakhmedov, S. S.; Shurukhina, A. V. Effect of intermolecular hydrogen bonding and proton transfer on fluorescence of salicylic acid. *J. Mol. Struct.* **1997**, *436*−*437*, 153−160.
(50) Selkoe, D. J. Imaging Alzheimer's amyloid. *Nat. Biotechnol.* **2000**, *18*, 823−824.
(51) Kung, M. P.; Hou, C.; Oya, S.; Mu, M.; Acton, P. D.; et al. Characterization of [^{123}I]IDAM as a novel single-photon emission tomography tracer for serotonin transporters. *Eur. J. Nucl. Med.* **1999**, *26*, 844−853.
(52) Munson, P. J.; Rodbard, D. LIGAND: a versatile computerized approach for characterization of ligand binding system. *Anal. Biochem.* **1980**, *107*, 220−239.

JM010045Q